Controlling the Topology of Fermi Surfaces in Metal Nanofilms

M. Ogawa,[1] A. Gray,[2] P. M. Sheverdyaeva,[3] P. Moras,[3] H. Hong,[4] L.-C. Huang,[5] S.-J. Tang,[5] K. Kobayashi,[6] C. Carbone,[3] T.-C. Chiang,[2] and I. Matsuda[1,*]

[1]*Institute for Solid State Physics, University of Tokyo, 5-1-5 Kashiwanoha, Kashiwa, Chiba 277-8581, Japan*
[2]*Department of Physics, University of Illinois, 1110 West Green Street, Urbana, Illinois 61801-3080, USA*
[3]*Istituto di Struttura della Materia, Consiglio Nazionale delle Ricerche, Trieste, Italy*
[4]*Advanced Photon Source, Argonne National Laboratory, 9700 South Cass Avenue, Argonne, Illinois 60439, USA*
[5]*Department of Physics and Astronomy, National Tsing Hua University, Hsinchu 30013, Taiwan*
[6]*Department of Physics, Faculty of Science, Ochanomizu University, 2-1-1 Otsuka, Bunkyo-ku, Tokyo 112-8610, Japan*

(Received 20 March 2012; published 13 July 2012)

The properties of metal crystals are governed by the electrons of the highest occupied states at the Fermi level and determined by Fermi surfaces, the Fermi energy contours in momentum space. Topological regulation of the Fermi surface has been an important issue in synthesizing functional materials, which we found to be realized at room temperature in nanometer-thick films. Reducing the thickness of a metal thin film down to its electron wavelength scale induces the quantum size effect and the electronic system changes from three to two-dimensional, transforming the Fermi surface topology. Such an ultrathin film further changes its topology through one-dimensional (1D) structural deformation of the film when it is grown on a 1D substrate. In particular, when the interface has 1D metallic bands, the system is additionally stabilized by forming an electron energy gap by hybridization between 1D states of the film and substrate.

DOI: 10.1103/PhysRevLett.109.026802 PACS numbers: 73.22.−f, 79.60.Dp

A Fermi surface, which is an energy contour in momentum space for electrons at the Fermi level, provides important information to understand the solid-state properties of metal crystals such as electron transport and phase transitions. The shapes of Fermi surfaces have been topologically categorized [1] and electronic phenomena, e.g., Peierls transitions, and quantities, e.g., Berry's phase, exist that are specific to each topological rank. The Fermi surface topology can be varied by changing the dimensionality of an electron system. For example, while a Fermi surface is a sphere for the three-dimensional (3D) free electron model, it is a circle in two dimensions, and two points in one dimension. On the other hand, the topology can also differ between closed and open Fermi surfaces. While the closed loop, such as a Fermi circle, only allows circular motion of an electron in a magnetic field, the open trajectory, e.g., a Fermi line, corresponds to infinite motion, which gives different Berry's phases for conducting electrons [1].

In this Letter, we regulate the Fermi surface topology, namely the electronic topological transition [1,2], for metal thin films on semiconductor substrates. As the thickness of a bulk metal crystal is scaled down to the order of its Fermi wavelength, the electronic system changes from being 3D to 2D by the quantum size effect [3]. Such variation of the dimensionality shifts the topological rank accordingly. Moreover, the ultrathin metal film in the quantum regime further changes its topology through the interface atomic layer. We observed the electronic topological transition, opening of the Fermi surfaces, by introducing a 1D array of indium (In) atomic chains with a 1-nm period into the interface [4] between a 2D silver (Ag) film with a thickness of 1 nm and a semiconducting silicon (Si) substrate. Because this demonstration has been carried out on metal films with a thickness of several atomic layers at room temperature, the results of this Letter develop both the topological physics and quantum devices in atomic-scale systems.

Electronic structure and atomic structure of the film were examined by angle-resolved photoemission and x-ray diffraction (XRD) measurements at the VUV-photoemission beam line [5] at Elettra (Trieste, Italy) and beam line 33-ID-E [6] at Advanced Photon Source (Argonne, IL, USA), respectively. At each beam line station, an experimental chamber system is equipped with metal evaporators, enabling *in situ* measurements of the samples prepared in ultrahigh vacuum. A Si(111)-(4×1)-In surface [4] was prepared by depositing In on a Si(111)-(7×7) clean surface at 350 °C. To prepare a single-domain surface, we used a vicinal Si wafer (n-type 2–15 Ω cm), whose normal was 1.8° off from (111) toward the $[\bar{1}\,\bar{1}\,2]$ direction. Ultrathin Ag(111) films were epitaxially formed by depositing Ag below 150 K on the Si(111)-(4×1)-In and Si(111)-(7×7) surfaces, followed by postannealing at room temperature [7–9]. Film thickness of Ag was determined by thickness monitor and a completion of the $\sqrt{3} \times \sqrt{3}$-Ag phase on Si(111). Crystallinity of films and surface superstructures was confirmed by electron diffraction.

Figure 1 shows an in-plane (k_x, k_y) photoemission intensity map at the Fermi level for Ag(111) films on a Si(111) substrate with (a) a 2D 7×7 surface phase, and (b),(c) a (4×1)-In surface phase [8] composed of an array

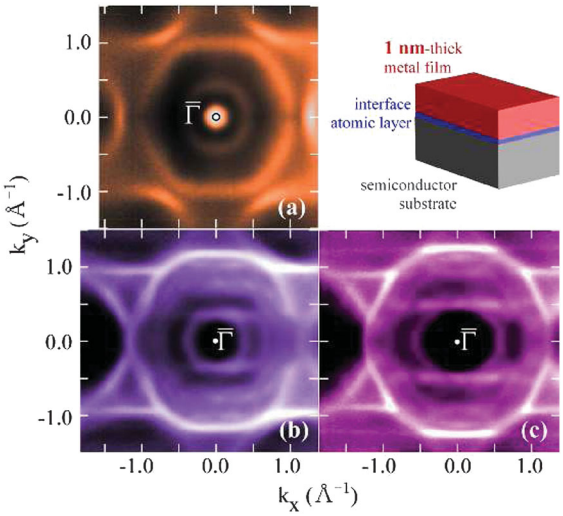

FIG. 1 (color). In-plane (k_x, k_y) photoemission intensity map at the Fermi level for (a) 1.4-nm (6 ML) thick Ag(111) film on Si(111)-(7 × 7), (b) 1.4-nm (6 ML) thick, and (c) 0.7-nm (3 ML) thick Ag films on Si(111)-(4 × 1)-In, measured at $h\nu = 50$ eV at room temperature. The difference is due to the change of an atomic layer at the interface between the metal film and semiconductor substrate. The brightness is proportional to the intensity of photoemission.

of atomic In chains with a period of $a_{\mathrm{int}} = 1.3$ nm. In this Letter, the x and y axes are defined as perpendicular and parallel to the directions of the In chain, respectively. Ag thickness is 6 monolayers (MLs, where 1 ML = 2.36 Å) in Figs. 1(a) and 1(b) and 3 ML in Fig. 1(c). The films were thin enough to induce the quantum confinement effect along the surface normal (z axis), so electronic states in the film are purely 2D. All of the bands in Fig. 1 belong to the quantum-well states (QWSs) [3,7,9–13] except for a Ag(111) surface state [14] at $\bar{\Gamma}$. In contrast to the isotropic contours for the film with the 2D film-substrate interface in Fig. 1(a), strong 1D anisotropy is clearly observed for those with a 1D atomic layer at the interface in Figs. 1(b) and 1(c).

Figures 2(a)–2(c) trace energy contours at the Fermi level from the photoemission maps of the QWS subbands in the Ag nanofilms. For the film on Si(111)-(7 × 7), the Fermi surfaces are a circle and hexagons for QWSs with quantum numbers of $n = 1$ and $n = 2$–5, respectively. Therefore, the contours are rings and have only closed components. On the other hand, the 1D anisotropic energy contours for the 6- and 3-ML thick Ag films grown on the Si(111)-(4 × 1)-In surface contain open sections. This indicates a change of the topological rank. As a result, the QWSs in the ultrathin film system exhibit electronic topological transitions due to the interface atomic layer.

Focusing on the $n = 1$ QWS subbands at $\bar{\Gamma}$ for the 6 ML film in Fig. 2(b), the shape of the Fermi surfaces is 1D curves (open Fermi surface) and a periodic array of ellipsoids (closed Fermi surfaces) along the k_x axis (see

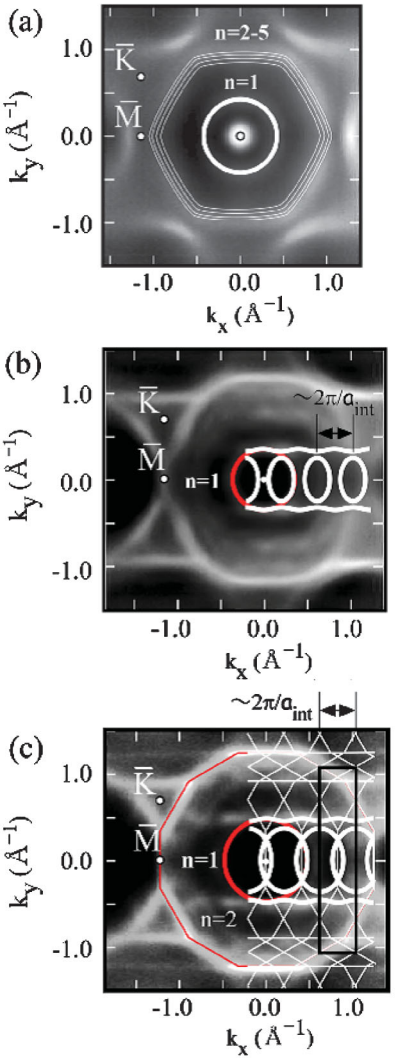

FIG. 2 (color). (a)–(c) Photoemission intensity maps in Fig. 1, superimposed by white traces of observed contours for the QWS subbands. In (b) and (c), the unperturbed Fermi surfaces of the films without 1D modulation are shown in red (dark gray). The unit cell is shown as a rectangle in (c).

Supplemental Material [15]). For the 3 ML film, the photoemission map in Fig. 2(c) is overlapped schematically by the original two Fermi rings, a circle for $n = 1$ and a dodecagon for $n = 2$, arranged in rows with the $2\pi/a_{\mathrm{int}}$ period along the k_x direction. The experimental intensity map is reproduced when one introduces anticrossing at the intersection between the two adjacent Fermi circles and crossing between the other combinations of the rings. For the $n = 1$ QWS subband, the original closed circle has changed into two open lines and a closed chain. It is of note that these 1D intensity lines are not simply a result of Fermi level crossing of the $n = 1$ QWS band, as described further below. In contrast to the rest of the QWS subbands in this Letter, the 1D band shows an electronic feature that is specific to this topology.

During the growth of an ultrathin film, it interacts structurally and electronically with the substrate [16].

The additional 1D potentials in the Ag films are likely to be related to these interactions. The atoms in the film rearrange to match the substrate lattice, while the electronic states in the film hybridize with those in the substrate. Starting with the structure effect, it has been found by scanning tunneling microscopy (STM) observation and theoretical calculations that a 6-ML thick Ag film on Si(111)-(4 × 1)-In contains periodic stacking faults inside the film [8,15,17]. This is caused by the distinctive difference in lattice structure between a face-centered cubic (fcc) Ag(111) crystal film and the Si(111)-(4 × 1)-In surface. Here, the film undergoes structural deformation to match the periodicity of the substrate.

To examine the atomic structure of the films, XRD measurements were carried out. A 2D profile of XRD pattern for the film in Fig. 3(a), measured along H (k_x) and L (k_z) directions at $h\nu = 19.9$ keV, is reproduced by a model with the stacking faults in Fig. 3(c), as indicated by red arrows. On the other hand, the 3-ML thick Ag film/(4 × 1) − In/Si(111) system in Fig. 3(b) shows that the film structure does not contain any stacking faults, as confirmed by the absence of the corresponding XRD signals. However, it is also different from the genuine fcc structure shown in Fig. 3(d). The existence of 1D structural modulation of a 3 ML film has been confirmed by observing a 1D periodic structure by STM [8], and by streaks in the electron diffraction pattern in this work. These results indicate that the 1D structures in the 6- and 3-ML thick films on Si(111)-(4 × 1)-In are distinctive.

Turning our attention to the electronic structure, prominent features in the Fermi surfaces are the appearance of a 1D line in the intensity map at $k_{F,y} = 0.3$ and 0.5 Å^{-1} for 6 and 3 ML films, respectively. Dispersion curves of the 1D bands, originating from the $n = 1$ QWS subband, are shown along the k_y axis at the selected k_x points in Fig. 4. The Fermi level crossings of the bands for the 6 ML film occur at $k_{F,y}^{n=1}$, indicated by arrows, in Figs. 4(a) and 4(b). In contrast, the edges of the Fermi level appear at $k_{F,y}^{n=1}$ for the 3 ML film in Figs. 4(d) and 4(e). If these 1D Fermi lines consist only of the QWS subbands in the 1D modulated films, the dispersion along the k_y axis must be parabolic and form a 1D electron pocket over the k_x axis, as shown in Fig. 4(g). Thus, the 1D dispersion curve for the 3-ML thick Ag film on Si(111)-(4 × 1)-In is extraordinary. On the other hand, it is known from previous photoemission research [4] that the Si(111)-(4 × 1)-In surface has 1D metallic bands with the Fermi vector at $k_{F,y} \sim 0.5$ Å^{-1}, forming a hole pocket over the k_x axis [Fig. 4(h)]. Therefore, as shown in Fig. 4(i), it is naturally deduced that these two 1D metallic bands hybridize with each other and eventually form an energy gap (ΔE) at $k_{F,y} \sim 0.5$ Å^{-1}, and the 1D photoemission lines of the 3 ML film in Fig. 2(c) correspond to the topmost or hole pockets of such a 1D hybrid band. In Fig. 2(c), a photoemission intensity line is also observed at $k_{F,y} = 1.2$ Å^{-1}. This 1D spectral feature is part of the Fermi surfaces of the $n = 2$ QWS subband in the 3-ML thick Ag film. The dispersion curve of the 1D state along the $\bar{M} - \bar{K}$ line, as presented in Fig. 4(f), shows a clear Fermi level

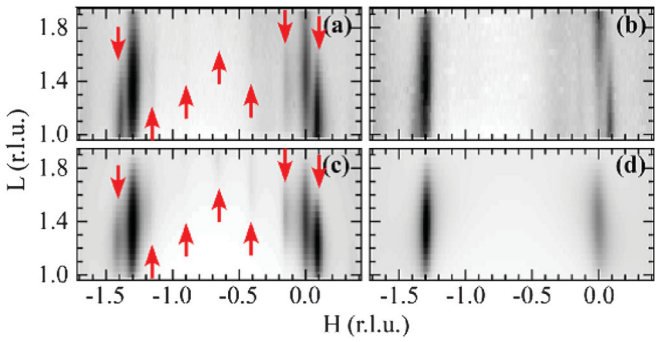

FIG. 3 (color). 2D intensity maps of 19.9 keV x ray in reciprocal space (H, $K = 1.33$, L). The data in (a) and (b) are experimental results obtained at room temperature on (a) 6-ML thick and (b) 3-ML thick Ag films on Si(111)-(4 × 1)-In, while those in (c) and (d) are simulations of a 6-ML thick fcc-Ag(111) film with and without stacking faults, respectively. The red arrows point to the same diffraction spots found in (a) and (c). The reciprocal lattice units (r.l.u.) are defined by the fundamental length of the Si(111)-(1 × 1) reciprocal vector. H and L are along x and z directions, respectively. K is along the ⟨112⟩ symmetry axis, which is rotated by 30° by the y direction.

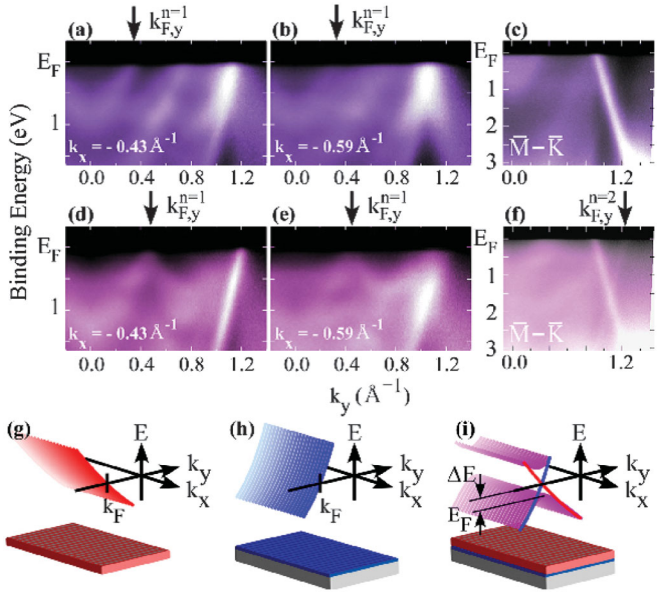

FIG. 4 (color). (a–f) Photoemission band diagrams of (a)–(c) 6-ML thick, and (d)–(f) 3-ML thick Ag films on Si(111)-(4 × 1)-In along the k_y axis at the selected k_x points and at the $\bar{M} - \bar{K}$ line. The $k_{F,y}$ points of the 1D Fermi lines of the intensity maps in Figs. 2 and 3 are indicated by arrows. (g)–(i) Schematic diagrams for modeling 1D band dispersion curves for the (g) 3-ML thick Ag film, (h) Si(111)-(4 × 1)-In substrate, and (i) 1D modulated Ag(111)/Si(111)-(4 × 1) − In system.

crossing and intersects with the adjacent $n = 2$ QWS band. This feature was not found for the 6 ML film, as shown in Fig. 4(c), indicating that the two films possess different electronic structures. From these results, the mechanisms of the transitions at thicknesses of 3 and 6 ML are distinctive in terms of both atomic and electronic structures. It is worth noting that the minimum thickness for an atomically flat Ag film is 3 ML on a Si(111)-(4 × 1)-In surface, while it is 6 ML on a Si(111)-(7 × 7) surface. Ag films with a thickness of 6 ML have successfully been described by the so-called electronic growth model on various semiconductor surfaces [18,19]. Thus, another mechanism is needed to explain the formation of the 3 ML Ag film on Si(111)-(4 × 1)-In. It is inferred from the present results that the system is electronically stabilized by the 1D energy gap opening at the Fermi level, which is shown as ΔE in Fig. 4(i). We emphasize that the present observation reveals an intriguing topological property that the 2D metal film has introduced into itself a 1D structural deformation to form 1D electronic states, and that the total system is electronically stabilized by hybridization with the 1D electronic states at the interface atomic layer.

In summary, we report that a 1-nm thick Ag crystal film on a semiconductor substrate exhibits a topological transition upon changing the interface atomic layer from a 2D clean surface to a periodic array of In atomic chains. The present results demonstrate, by focusing on individual QWS subbands, that the Fermi surfaces can be varied from closed to open. Thus, by choosing films with an appropriate combination of material and substrate, the Fermi surface topology can be controlled. Transport experiments of the film prepared by the present process will allow for studying various issues in topology physics, e.g., the observation of anisotropic electric conduction, the variation of Berry's phase, and examination of the Novikov conjecture [1]. It is worth noting that measurements of such nanofilms have now become possible using microscopic probes [20,21].

This work was funded by (1) JSPS (KAKENHI 18360018), (2) Italian MIUR Grant No. PRIN 20087NX9Y, (3) Executive Program of Cooperation in the Fields of Science and Technology between the Government of Italy and the Government of Japan, and (4) the U.S. Department of Energy, Office of Science, Office of Basic Energy Sciences, under Contract No. DE-AC02-06CH11357 (operations of APS) and Grant No. DE-FG02-07ER46383 (T.-C. C.). The supporting experiment at the Photon Factory was performed at BL-18A under Grant No. 2008G100. Naoka Nagamura, Osamu Sugino, and Takashi Uchihashi are acknowledged for their valuable comments.

*imatsuda@issp.u-tokyo.ac.jp

[1] *Topology in Condensed Matter* edited by M. I. Monastyrsky (Springer-Verlag, Berlin, 2006).
[2] A. E. Meyerovich and D. Chen, Phys. Rev. B **66**, 235306 (2002).
[3] T.-C. Chiang, Surf. Sci. Rep. **39**, 181 (2000).
[4] H. W. Yeom, S. Takeda, E. Rotenberg, I. Matsuda, K. Horikoshi, J. Schaefer, C. M. Lee, S. D. Kevan, T. Ohta, T. Nagao, and S. Hasegawa, Phys. Rev. Lett. **82**, 4898 (1999).
[5] P. Moras, D. Topwal, P. M. Sheverdyaeva, L. Ferrari, J. Fujii, G. Bihlmayer, S. Blügel, and C. Carbone, Phys. Rev. B **80**, 205418 (2009).
[6] H. Hong and T.-C. Chiang, Nucl. Instrum. Methods Phys. Res., Sect. A **572**, 942 (2007).
[7] N. Nagamura, I. Matsuda, N. Miyata, T. Hirahara, S. Hasegawa, and T. Uchihashi, Phys. Rev. Lett. **96**, 256801 (2006).
[8] T. Uchihashi, C. Ohbuchi, S. Tsukamoto, and T. Nakayama, Phys. Rev. Lett. **96**, 136104 (2006).
[9] T. Okuda, Y. Takeichi, K. He, A. Harasawa, A. Kakizaki, and I. Matsuda, Phys. Rev. B **80**, 113409 (2009).
[10] N. Miyata, H. Narita, M. Ogawa, A. Harasawa, R. Hobara, T. Hirahara, P. Moras, D. Topwal, C. Carbone, S. Hasegawa, and I. Matsuda, Phys. Rev. B **83**, 195305 (2011).
[11] I. Matsuda, T. Ohta, and H. W. Yeom, Phys. Rev. B **65**, 085327 (2002).
[12] N. J. Speer, S.-J. Tang, T. Miller, and T.-C. Chiang, Science **314**, 804 (2006).
[13] S.-J. Tang, L. Basile, T. Miller, and T.-C. Chiang, Phys. Rev. Lett. **93**, 216804 (2004).
[14] S. Hüfner, *Photoelectron Spectroscopy* (Springer-Verlag, Berlin, 2003).
[15] See Supplemental Material at http://link.aps.org/supplemental/10.1103/PhysRevLett.109.026802 for a simulated Fermi surface for the 6 ML Ag film on the Si(111)-(4 × 1) surface.
[16] S.-J. Tang, C.-Y. Lee, C.-C. Huang, T.-R. Chang, C.-M. Cheng, K.-D. Tsuei, H.-T. Jeng, V. Yeh, and T.-C. Chiang, Phys. Rev. Lett. **107**, 066802 (2011).
[17] K. Kobayashi and T. Uchihashi, Phys. Rev. B **81**, 155418 (2010).
[18] Z. Zhang, Q. Niu, and C.-K. Shih, Phys. Rev. Lett. **80**, 5381 (1998).
[19] I. Matsuda, H. W. Yeom, T. Tanikawa, K. Tono, T. Nagao, S. Hasegawa, and T. Ohta, Phys. Rev. B **63**, 125325 (2001).
[20] N. Miyata, R. Hobara, H. Narita, T. Hirahara, S. Hasegawa, and I. Matsuda, Jpn. J. Appl. Phys. **50**, 036602 (2011).
[21] T. Kanagawa, R. Hobara, I. Matsuda, T. Tanikawa, A. Natori, and S. Hasegawa, Phys. Rev. Lett. **91**, 036805 (2003).